

Towards a Larger Molecular Simulation on the Quantum Computer: Up to 28 Qubits Systems Accelerated by Point Group Symmetry

Changsu Cao,^{1,2} Jiaqi Hu,³ Wengang Zhang,^{1,3,4} Xusheng Xu,¹ Dechin Chen,¹
Fan Yu,¹ Jun Li,^{2,5} Hanshi Hu,^{2,*} Dingshun Lv,^{1,†} and Man-Hong Yung^{1,3,4,‡}

¹Central Research Institute, 2012 Labs, Huawei Technologies

²Department of Chemistry, Tsinghua University, Beijing 100084, China

³Department of Physics, Southern University of Science and Technology, Shenzhen 518055, China

⁴Shenzhen Institute for Quantum Science and Engineering, Southern University of Science and Technology, Shenzhen 518055, China

⁵Department of Chemistry, Southern University of Science and Technology, Shenzhen 518055, China

(Dated: September 7, 2021)

The exact evaluation of the molecular ground state in quantum chemistry requires an exponential increasing computational cost. Quantum computation is a promising way to overcome the exponential problem using polynomial-time quantum algorithms. A quantum-classical hybrid optimization scheme known as the variational quantum eigensolver (VQE) is preferred for this task for noisy intermediate-scale quantum devices. However, the circuit depth becomes one of the bottlenecks of its application to large molecules of more than 20 qubits. In this work, we propose a new strategy by employing the point group symmetry to reduce the number of operators in constructing ansatz to achieve a more compact quantum circuit. We illustrate this methodology with a series of molecules ranging from LiH (12 qubits) to C₂H₄ (28 qubits). A significant reduction of up to 82% of the operator numbers is reached on C₂H₄, which enables the largest molecule ever simulated by VQE to the best of our knowledge.

I. INTRODUCTION

Obtaining the accurate ground state and its corresponding energy of the many-electrons molecular system is of great importance. In recent decades, a variety of post-Hartree-Fock methods such as configuration interaction (CI) and coupled cluster (CC) have been proposed and applied to achieve quantitatively satisfying results while at the expense of exponentially growing complexity with the system size. Such complexity hinders the applications to larger molecular systems.

Quantum computing is proposed to be a promising way to overcome the exponential issue, as speculated by Feynman in 1982 [1]. Since then, various quantum algorithms have been developed for simulations [2–5]. Among them, the variational quantum eigensolver (VQE) [5–7] is believed to be friendly to near-term quantum devices for its noise-resilient property and a small need for quantum gates [8]. VQE is a hybrid quantum-classical variational algorithm, where the quantum computer prepares the ansatz and measures the quantum state, while the classical computer gathers the measurement results, optimizes the parameters, and sends them back to the quantum computer. Since the first H₂ (2 qubits) demonstration presented in Ref. [5], there have been a variety of experiments to apply VQE for small molecule systems, like BeH₂ (6 qubits) [9], H₂O (8 qubits) [10] and H₁₂ (12 qubits) [11]. There also have been some results benchmarking the performance of VQE by quantum simulators [12–14]. To date, the largest qubit number used in numerical simulation of molecule systems was 20 qubits for H₂O [13].

Recent results of VQE show an optimistic prospect of it.

For larger systems, however, the results of the VQE simulation are still absent. One important reason for the limited simulation size is that a scalable ansatz whose parameter space covers the unknown ground state of the targeted system remains to be found. Thus, a variety of works have focus on designing different types of ansatz in VQE [15–18], which is believed to save resources when simulating other systems.

To simulate larger molecule systems by VQE, one crucial direction is to decrease the operator number in ansatz. Since VQE has been proposed initially using UCC ansatz, there have been many efforts to reduce the number of operators in it. For example, using classical pre-calculation to screen out the terms that are small enough [19]; Similarly, by chemical intuition, only choosing the important excitation operators [18] or only using paired double excitation operators in ansatz [20] or the recently proposed energy sort based scheme [21]. However, these methods are approximate, which limited their application scenarios. It will be more convincing to improve UCC type ansatz based on built-in information of the molecules.

As an attempt, there have also been some works using the molecule's symmetry to reduce quantum resources. Symmetric properties in molecular systems such as the particle number conservation ($U(1)$ symmetry), the fermionic parity conservation (Z_2 symmetry), are used to be restrictions in VQE [22–24]. The spatial symmetry, i.e. the point group symmetry, is also a fundamental property of the molecular system. It provides amounts of intrinsic information of the geometric and the electronic structures of the certain molecule and has been widely used in the community of theoretical and computational chemists([25, 26]). Applications of point group symmetry in VQE have also been realized in some work. For example, using point group symmetries as Pauli operators to taper off the number of qubits [27], simplify Hamiltonian [28, 29], or run VQE in subspace [30]; symmetry configuration mapping (SCM) method [31].

* hshu@mail.tsinghua.edu.cn

† ywlds@163.com

‡ yung.manhong@huawei.com

Instead, in this work, we use the point group symmetry to directly reduce the UCC ansatz operator so that the depth of the quantum circuit is significantly decreased without sacrificing accuracy. We present a series of numerical cases with the symmetry reduced unitary coupled-cluster singles and double (SymUCCSD) ansatz by the MindQuantum simulator, including LiH, HF, H₂O, BeH₂, CH₄, and NH₃ with its flipping potential energy surface. We also successfully performed the simulation of 28 qubits C₂H₄, to the best of our knowledge, the largest size in qubits ever simulated via UCCSD-VQE.

The article is structured as follows: we start by reviewing the formalism of the VQE and UCCSD ansatz in Section II. We then describe the ansatz reduction by the point group symmetry in Section III. After that, the numerical examples with a series of molecules at both equilibrium and non-equilibrium geometries are demonstrated in Section IV.

II. VQE METHOD

The variational quantum eigensolver (VQE) method is originally designed to solve the ground state energies of molecular Hamiltonian [6]. Typically, in these problems, the Hamiltonian under Born-Oppenheimer approximation is usually written in a second-quantized form [32] as

$$\hat{H} = \sum_{p,q} h_{pq} \hat{a}_p^\dagger \hat{a}_q + \frac{1}{2} \sum_{p,q,r,s} g_{pqrs} \hat{a}_p^\dagger \hat{a}_r^\dagger \hat{a}_s \hat{a}_q, \quad (1)$$

where \hat{a}_p^\dagger and \hat{a}_p denote the fermionic creation operator and annihilation operator associated with p -th fermionic mode (or spin-orbital), etc. The sets of coefficients $\{h_{pq}\}$ and $\{g_{pqrs}\}$ are called one- and two-electron integrals and can be evaluated by classical computers.

The idea of the VQE is to use the variational method to approximate the ground state of a given Hamiltonian. The essential part of VQE is to prepare the ansatz by parameterized quantum circuits which should be close to the unknown ground state. The variational principle can be written as

$$\frac{\langle \Psi(\theta) | \hat{H} | \Psi(\theta) \rangle}{\langle \Psi(\theta) | \Psi(\theta) \rangle} = \langle E \rangle \geq E_{gs}, \quad (2)$$

where $\langle E \rangle$ is the expectation value of Hamiltonian \hat{H} , and E_{gs} is the exact ground state energy. From it, one can obtain the ground state energy in the desired accuracy after optimization if a proper ansatz is chosen.

To date, different methods for constructing the ansatz for VQE have been proposed. Among them, the UCC ansatz is one that was being focused on from the very beginning of the VQE study [33]. The UCC ansatz is originated from coupled cluster(CC) operators and can be written as

$$|\Psi(\theta)\rangle = e^{\hat{T}(\theta) - \hat{T}^\dagger(\theta)} |\Psi_0\rangle = \hat{U}(\theta) |\Psi_0\rangle, \quad (3)$$

where $|\Psi_0\rangle$ is a reference state, $\hat{T}(\theta)$ is the cluster operator and can be written as

$$\hat{T}(\theta) = \sum_k \hat{T}_k(\theta) \quad (4)$$

where $\hat{T}_k(\theta)$ are excitation operators with different orders like

$$\hat{T}_1(\theta) = \sum_{i,a}^{a \in \text{vir}, i \in \text{occ}} \hat{t}_i^a = \sum_{i,a}^{a \in \text{vir}, i \in \text{occ}} \theta_i^a \hat{a}_a^\dagger \hat{a}_i \quad (5)$$

$$\hat{T}_2(\theta) = \sum_{i,j,a,b}^{a,b \in \text{vir}, i,j \in \text{occ}} \hat{t}_{ij}^{ab} = \sum_{i,j,a,b}^{a,b \in \text{vir}, i,j \in \text{occ}} \theta_{ij}^{ab} \hat{a}_a^\dagger \hat{a}_b^\dagger \hat{a}_i \hat{a}_j \quad (6)$$

and so on. Here \hat{a} and \hat{a}^\dagger are annihilation and creation operators. The adjustable parameter series of θ work as variables in the variational algorithm. Noticing that the form $\hat{U}(\theta) = e^{T(\theta) - T^\dagger(\theta)}$ guarantees the operator to be unitary. If truncate Eq. 4 to $k = 2$, it is called UCCSD.

To prepare the ansatz operator $\hat{U}(\theta)$ in a quantum computer, one can transform it into a set of Pauli words in the exponent. This transform can be done by Jordan-Wigner(JW) [34] transformation, which can write as

$$\begin{aligned} \hat{a}_j^\dagger &= \frac{1}{2} (\hat{\sigma}_j^x + i \hat{\sigma}_j^y) \left(\bigotimes_{i=1}^{j-1} \hat{\sigma}_i^z \right) \\ a_j &= \frac{1}{2} (\hat{\sigma}_j^x - i \hat{\sigma}_j^y) \left(\bigotimes_{i=1}^{j-1} \hat{\sigma}_i^z \right), \end{aligned} \quad (7)$$

where $\hat{\sigma}_j^x, \hat{\sigma}_j^y, \hat{\sigma}_j^z$ are Pauli operators that will apply to the j -th qubit. If using the JW transformation, the fermionic modes are naturally mapped to the qubits, noticing that the qubit number needed to scale linearly to the fermionic modes. The transformed operators can be decomposed into quantum gates by Trotterization [35]. Then the parameters in the operators will be adjusted by adjustable parameters in quantum gates, like the single-qubit rotation angles. Finally, these gates will apply to the qubits to prepare the ansatz.

To make the expectation value in Eq. 2 as small as possible, in practice, VQE usually combines classical optimization methods to do variational steps. All the Pauli expectation values needed in optimization will be measured in a quantum computer, and the measurement cost could be reduced by the recently proposed advanced measurement schemes [36–39]. Then these values will be used to calculate expectation, gradient, etc, and perform optimization in a classical computer, and generate a new set of parameters according to the optimizer used to update the ansatz. This process will be done repeatedly until the optimization converges to the ground state energy.

III. SYMMETRY REDUCTION

The point group symmetry has been employed in quantum chemistry to simplify the calculation and integral, which significantly saving computation resources. The amplitude (and also the one- and two-electron integrals) in the expression of coupled cluster (CC) will vanish unless the corresponding term preserves the totally symmetric irreducible representation (of which the characters are all 1), which has been

proved decades ago. Čársky et.al. [25] first applied the point group system in coupled-cluster double (CCD) method to simplify the calculation. Stanton et.al. [26] further improve it to the general coupled-cluster and many-body perturbation theory (MBPT).

However, in the UCC method, the excitation operators in the exponent can not be expressed with finite terms, it is not obvious whether the point group symmetry constraint is still valid. We prove in the Appendix that the constraint of the point group symmetry still preserves in the UCC. So that the expansion of the unitary coupled cluster wavefunction will only contain the terms with the same irreducible representation (*irrep*) as the reference wavefunction.

Here we take molecule BeH₂ as an example. The point group for BeH₂ is D_{2h}, which has eight irreducible representations D , i.e. $D \in \{A_g, B_{1g}, B_{2g}, B_{3g}, A_u, B_{1u}, B_{2u}, B_{3u}\}$. For the simple closed shell molecules like BeH₂ (meaning there is no unpaired electron), the ground state is necessarily to be of the totally symmetric irrep, i.e. A_g in D_{2h} group. This conclusion applies to most of the organic compounds and simple ionic compounds including all the cases listed in this work. However, when it comes to molecules with unpaired electrons, the irrep of the ground state can not get determined directly. In such situations, the ground state evaluated by Hartree-Fock is a good starting point and usually predicts the correct irrep of the true ground state. For more complex cases where a single Slater determinant is not a good approximation, multiple attempts of the Hartree-Fock ground state and low lying excited states may be needed for reaching the true ground state.

Suppose the reference wavefunction $|\Psi_0\rangle$ of BeH₂ is a Slater determinant evaluated by Hartree-Fock. As we presented in VIB, the exponent operator will not change the irrep A_g of the reference Hartree-Fock wavefunction $|\Psi_0\rangle$. So the targeted unitary coupled cluster solution $|\Psi\rangle$ of BeH₂ constructed from $|\Psi_0\rangle$ is of the same irrep A_g as well and the expansion of $|\Psi\rangle$ to Hartree-Fock Slater determinants will contain only the terms of A_g irrep. In our implementation, we filter out the operators with undesirable irrep when constructing the UCC ansatz.

For example, the single exciting operator is divided into eight parts according to the irrep of $\hat{t}|\Psi_0\rangle$,

$$\hat{T}_1(\hat{\theta}) = \sum_{irrep \in D} \left(\sum_{i,a} \theta_a^i \hat{a}_a^\dagger \hat{a}_i \right)_{irrep}. \quad (8)$$

To keep the invariance of irrep, in the exciting operator, we have

$$\sum_{\substack{B_{1g}, B_{2g}, B_{3g}, \\ A_u, B_{1u}, B_{2u}, B_{3u}}} \left(\sum_{i,a} \theta_a^i \hat{a}_a^\dagger \hat{a}_i \right)_{irrep} = 0. \quad (9)$$

Only the terms excite $|\Psi_0\rangle$ to A_g states remain, and the rest of the terms in the exciting operator are excluded in constructing the cluster operator.

In general, it is represented as

$$\forall D(\hat{t}|\Psi_0\rangle) \neq D(|\Psi_0\rangle) : \hat{t} = 0, \quad (10)$$

where D is the irrep of the corresponding wavefunction. By this method, a large number of terms in Eq. 8 can be eliminated. With the filtered operator, the number of parameters and the depth of the quantum circuit are significantly reduced. The whole scheme of the symmetry reduced VQE is summarized in Algorithm 1.

Algorithm 1: Scheme of SymUCCSD in VQE

1. Initialize the reference state $|\Psi_0\rangle$ (Usually the Hartree-Fock ground state).
 2. **For** each possible excitation operator \hat{t}_k in \hat{T}
 - If** $D(\hat{t}_k|\Psi_0\rangle) \neq D(|\Psi_0\rangle)$
 - Remove \hat{t}_k from \hat{T} .
 - End**
 - End**
 3. Construct the ansatz operator $e^{\hat{T}-\hat{T}^\dagger}$ by the reduced \hat{T} .
 4. Convert the ansatz operator to the quantum circuit and prepare the ansatz.
 5. Perform VQE loop with the generated ansatz until the energy converges or reach the max number of iterations.
-

The key step of our method is to compare the irrep of all the possible excited states with the reference state. The wavefunction is expressed as the Slater-determinant of a collection of molecular orbitals, i.e. $|\Psi_0\rangle = |\phi_1 \bar{\phi}_1 \phi_2 \bar{\phi}_2 \dots \phi_n \bar{\phi}_n\rangle$, where ϕ is the occupied molecular spin-orbital and the bar indicates the different spin. Accordingly, the irrep of the wavefunction is determined from the direct product of the irrep of the molecular spin-orbitals by looking up the product table of irreps. Again, we take BeH₂ in D_{2h} as an example to illustrate it. In Fig. 1(a) we provide a product table for D_{2h} group, where the product relationship between two irrep in D_{2h} is given. Fig. 1(b-d) presents three different electronic configuration diagrams of BeH₂. In Fig. 1(b) we present the Hartree-Fock ground state, i.e. the reference state, in which three lowest orbitals with the irrep of a_g , b_{1u} and a_g are doubly occupied. By referring to the product table in Fig. 1(a), the irrep of the reference state is easily obtained, as $(a_g \otimes a_g) \otimes (b_{1u} \otimes b_{1u}) \otimes (a_g \otimes a_g) = a_g \otimes a_g \otimes a_g = A_g$. Usually, the irrep of the molecular wavefunction is written in uppercase to distinguish from the irrep of the molecular orbitals. In our method, after determining the irrep of the reference state, then all the possible single Slater-determinant excited terms $\hat{t}|\Psi_0\rangle$ are traversed to check whether their share the same irrep as the reference term. We present two specific examples in Fig. 1(c,d). For the single excitation term $\hat{t}_3^4|\Psi_0\rangle$ in Fig. 1(c), one electron is excited from the 3rd orbital to the 4th orbital. Its corresponding irrep is $(a_g \otimes a_g) \otimes (b_{1u} \otimes b_{1u}) \otimes (a_g) \otimes (b_{2u}) = a_g \otimes a_g \otimes a_g \otimes b_{2u} = B_{2u} \neq A_g$, which is not expected, and the exciting operator \hat{t}_3^4 should be excluded from constructing the cluster operator. As shown in Fig. 1(d), both two electrons at the 3rd orbital are excited from to the 4th orbital. The irrep is similarly evaluated as

$(a_g \otimes a_g) \otimes (b_{1u} \otimes b_{1u}) \otimes (b_{2u} \otimes b_{2u}) = a_g \otimes a_g \otimes a_g = A_g$, which is the same as the reference term. So the exciting operator \hat{t}_{33}^{44} is remained in constructing the cluster operator.

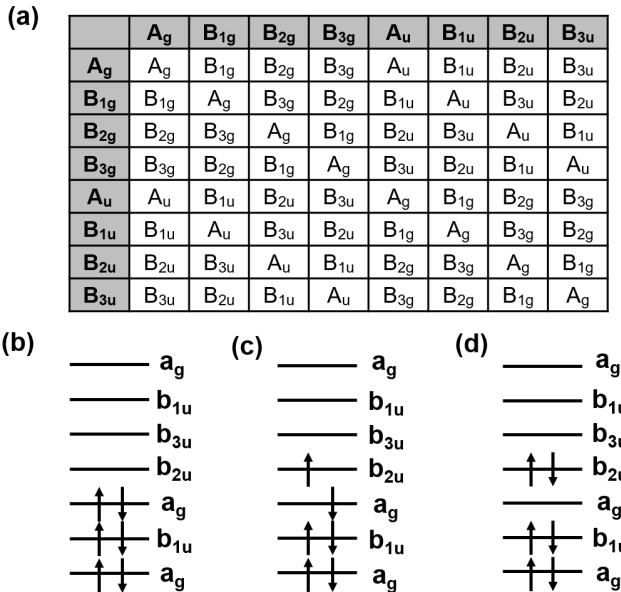


Fig. 1. **The irrep of the D_{2h} point group for a BeH_2 molecule.** (a) The product table for the irreducible representations of the D_{2h} group. (b) The electron configuration diagram of BeH_2 of the reference state, i.e. the Hartree-Fock state. (c) An example of coupled-cluster terms that corresponding to a configuration with different irrep compare to the reference state. This term is a single excitation concerning the reference term. (d) An example of coupled-cluster terms that corresponding to a configuration with the same irrep as the reference state. Note that it is conventionally to label the irrep of the molecular orbital in lower case like a_g and the irrep of the molecular state in upper case like A_g .

We apply this method to a series of molecules (without further VQE steps) and compare parameter numbers in ansatz before and after symmetry reduction in Fig. 2. The number of the parameters grows much slower after filtering out the symmetry forbidden terms. It is seen that the number of the parameters is impressively reduced and grows much slower after filtering out the symmetry forbidden terms, which means a shallower quantum circuit and fewer computational resources are needed now. For C_2H_4 , we reduced the coupled cluster terms from 1034 to 177, which is only around 17% of the terms before employing the symmetry constrain. Note that to apply the point group symmetry reduction, we only perform the VQE once. After constructing the reduced cluster operator, combining other reduction methods to further simplify the ansatz is also possible. [16, 21, 40, 41].

IV. NUMERICAL RESULTS

Using the symmetry reduction method mentioned above, we performed the symmetry reduced VQE-UCCSD on sev-

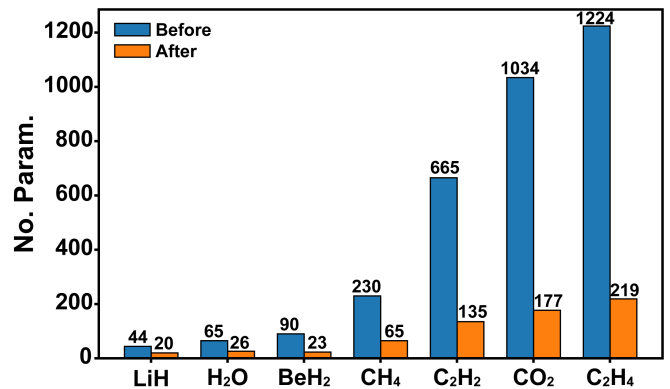


Fig. 2. **The number of parameters for a series of molecules before and after the reduction by point group symmetry.** We observed that the ratio of the necessary parameters decreases slightly as the size of the system increases, ranging from 25.6% of BeH_2 , to 20.3% of C_2H_2 and to 17.9% of C_2H_4 , all of which are of the same D_{2h} symmetry, indicating better efficient for larger molecules.

eral testing systems, varying from 12 qubits LiH to 28 qubits C_2H_4 . Specially, we simulated BeH_2 under various point group symmetry to study the relationship between the order of the group and the reduction of parameters. The flipping of ammonia, which involves the non-equilibrium geometry structures, was simulated as well. All the VQE simulations are performed using the quantum simulator MindQuantum [42] in the KunLun server with 1536 CPUs. STO-3G basis set was employed in all cases. The fermion operators are transformed to qubit type operators by Jordan-Wigner transformation [34]. Gradient-based optimization method BFGS is used to minimize the energy expectation value generated by the MindQuantum. All the geometric structures are obtained from CCCBDB-NIST Database [43].

A. BeH_2 : under different point group symmetries

A specific molecule belongs to different point groups at the same time, i.e. the point group with the highest symmetry and its subgroups. Here we simulate BeH_2 with various point groups assigned to study the relationship between the order of the group and the reduction of the ansatz. D_{2h} is the abelian point group with the largest order to which the geometry of BeH_2 belongs to. Alternatively, we can also take the subgroup of D_{2h} , i.e. D_2 , C_{2h} , C_{2v} , C_2 , C_s , C_i , and C_1 , to reduce the ansatz in Section III. After filtered by the constrain of the point group symmetry, the number of remaining parameters is approximately proportional to the reciprocal of the order of the group, $1/h$, as shown in Fig. 3. C_1 group, which is composed of the identity operation exclusively, has only the A irrep and means "no symmetry". Thus, under the C_1 group, our algorithm will not eliminate parameters and works exactly as the original VQE-UCCSD calculation. The 2nd order groups C_s , C_i , and C_2 include an additional one reflection (mirror plane), inversion (inversion center), or one rotation (rotation

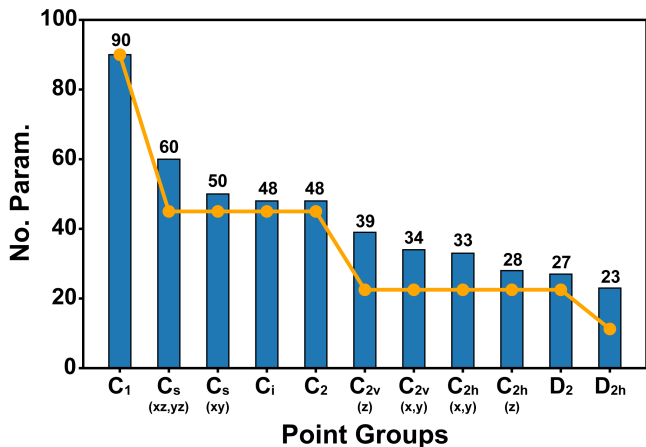


Fig. 3. **Parameters reduction of BeH_2 under various point group.** The orientation of the symmetry elements changes the ratio of reduction slightly. The orange line is the hypothetical situation that the number of configurations belongs to each irrep equal.

axis) operation, respectively. Around half of the parameters are filtered out when employing the 2nd order groups while the orientation of symmetry elements will affect the efficiency of the reduction. If we adopt the mirror in xy-plane (z-axis along with H-Be-H bond), more parameters will be cleaned than adopting the mirror in xz- or yz-plane. Similarly, the number of parameters is further reduced when applying the 4th order groups, C_{2v} , C_{2h} , and D_2 , and the 8th order group, D_{2h} . There is little promotion in the parameter reduction from the 4th order groups to the 8th order group D_{2h} . It is because the excited terms are distributed unevenly in each irrep especially in small systems. The uneven distribution problem will be improved when it comes to larger systems.

In general, the number and parameters are cut down to around $1/h$ of the original, where h is the order of the group and equals the number of irreps in a certain point group. It is agreed with the intuition that the more symmetric molecule is, the less resource it needs to simulate. The point group with larger orders will be more efficient in resource-saving, vice versa.

B. Simulations of small molecules

A variety of molecules, i.e. the hydrides containing the 2nd row elements, are chosen as the testing cases for benchmark, including LiH, HF, H_2O , BeH_2 , NH_3 , CH_4 . The equilibrium geometric structures are obtained from CCCBDB-NIST Database [43]. The UCCSD calculations with and without symmetry reductions are performed using the MindQuantum simulator. In addition, classical FCI and CCSD results calculated with PySCF are also provided [44, 45]. STO-3G basis sets are used for all cases.

In Table. I, we list the relevant information about the symmetry-reduced UCCSD (SymUCCSD) simulation of the

molecules mentioned above together with the reference to the energy calculated by original UCCSD, CCSD, and FCI. In our SymUCCSD calculations, the highest possible Abelian point group was chosen to simplify the ansatz. Among the testing molecules, the ratio of the remained parameters ranging from 26% in BeH_2 with D_{2h} to 56% in NH_3 with C_s . In the worst case that we tested, around half of the parameters are reduced as the lower bound for the symmetric molecular systems, corresponding to the half size of the quantum circuit. The energy calculated by SymUCCSD, UCCSD and CCSD results is compared to the FCI reference results. The differences are all less than 1.6 mHartree (chemical accuracy). So removing the unfavored operators in the UCCSD ansatz will not sacrifice the accuracy of the result, as supported by *Appendix.B* that the cluster operator should be totally symmetric and not change the symmetry of the reference wavefunction otherwise the generated coupled cluster wavefunction would not be the eigenvector of the Hamiltonian.

C. Ammonia Flipping

The molecule in the non-equilibrium geometry is important when studying the chemical reaction process which involves bond breaking and conformations changes. To explore the scenario of the non-equilibrium structures, we choose the ammonia flipping process to demonstrate our algorithm. The reaction coordination is computed using PBE density functional approximation [46] with def2-tzvp [47] basis set in PySCF [44, 45]. The energy profiles regarding FCI, CCSD and SymUCCSD methods are shown in Fig. 4. Concerning the flipping process, the C_s symmetry is kept so that the parameter reduction is the same as that in Table I.

When referring to the FCI results, the error increases when the structure turns from equilibrium to non-equilibrium geometries and reaches the maximum at the flat structure ($\angle z - N - H = 90^\circ$), $0.35m\text{Hartree}$ for CCSD and $0.33m\text{Hartree}$ for SymUCCSD. It agrees with our intuition that in the non-equilibrium structure, the multi-reference properties are not negligible anymore. FCI describes the multi-reference properties well, while the truncated CCSD and UCCSD are generally believed to be single-reference methods. The energies calculated by SymUCCSD are slightly lower than those by CCSD. It is probably attributed to the introducing of the de-excitation operator in UCC ansatz.

D. C_2H_4 : Large molecule simulation

To explore the limit of our method in the current simulator, we present here a simulation on 28 qubits C_2H_4 molecule, which becomes tractable after the reduction by our way. As shown in Fig. 5, the calculation converges after 25 iterations and reaches the chemical accuracy around 12th iteration. As shown in Fig. 2, the parameters for this ansatz are reduced from 1224 to 219. C_2H_4 belongs to D_{2h} point group. The symmetry of the total wavefunction is A_g irrep. Table. II shows that there are 48 single excitations and 1176 double

Table I. VQE simulations for small molecules. The simulation scale ranges from 12 to 18 qubits. The original parameters and the parameters after reduction show in the 4th and 5th columns. The number of parameters and the time used of the symmetry reduction ansatz compare to original UCCSD ansatz are shown in the 6th column. The energy differences compared with the FCI energy are shown in the last three columns with unit in Hartree. The equilibrium geometric structures of these molecules are obtained from CCCBDB-NIST Database [43].

| | Qubits | Sym. | Para.-Before | Para.-After | % | $\Delta E_{SymUCCSD}$ | ΔE_{UCCSD} | ΔE_{CCSD} |
|------------------|--------|----------|--------------|-------------|-----|-----------------------|-----------------------|-----------------------|
| HF | 12 | C_{2v} | 20 | 11 | 55% | 1.38×10^{-5} | 1.82×10^{-5} | 2.94×10^{-8} |
| LiH | 12 | C_{2v} | 44 | 20 | 45% | 1.09×10^{-5} | 1.10×10^{-5} | 1.05×10^{-5} |
| H ₂ O | 14 | C_{2v} | 65 | 26 | 40% | 1.09×10^{-4} | 1.19×10^{-4} | 1.17×10^{-4} |
| BeH ₂ | 14 | D_{2h} | 90 | 23 | 26% | 3.82×10^{-4} | 3.83×10^{-4} | 3.94×10^{-4} |
| NH ₃ | 16 | C_s | 135 | 75 | 56% | 1.86×10^{-4} | 1.94×10^{-4} | 2.14×10^{-4} |
| CH ₄ | 18 | D_2 | 230 | 105 | 46% | 1.96×10^{-4} | 2.06×10^{-4} | 2.30×10^{-4} |

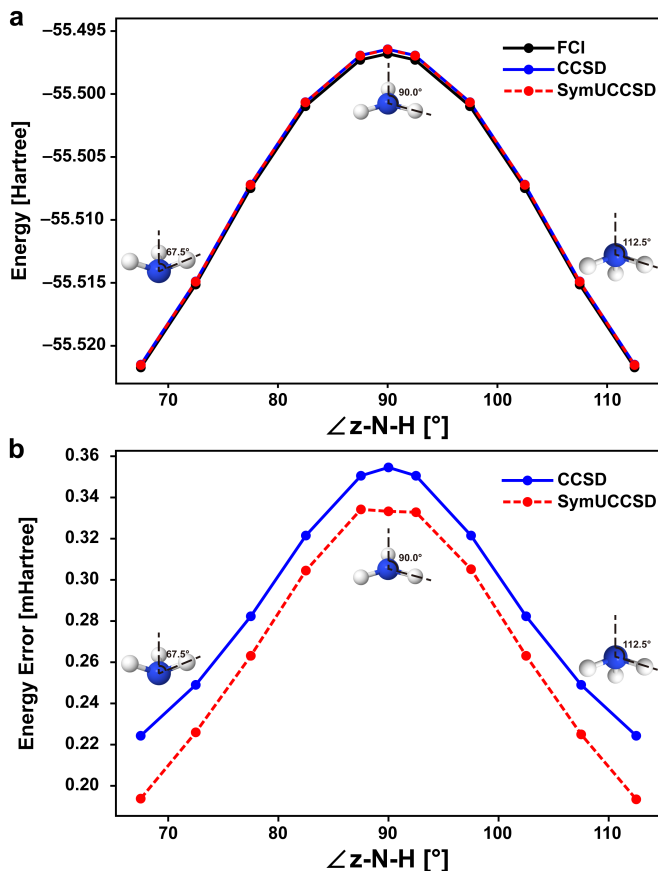


Fig. 4. **The potential energy curve of the ammonia flipping.** **a.** Potential energy surface calculated by FCI, CCSD, and the symmetry-reduced UCCSD during ammonia flipping; **b.** Energy error comparing with FCI energy. The flipping process is described by the angle of the z-axis, N atom and H atom. The unit of the error is mHartree.

excitations with the spin symmetry considered. Only the exciting configurations that belong to the same irrep as the reference wavefunction need to be included in the following VQE-UCCSD calculation. Only 18% of parameters remain after the symmetry reduction, which significantly shortens the depth of the circuit. The greatly reduced parameters are an important reason that makes such simulation tractable with the current quantum simulator.

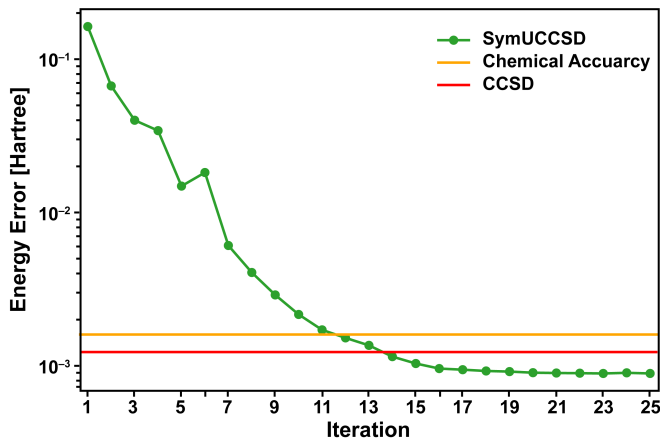


Fig. 5. **The convergence process of SymUCCSD for C₂H₄.** The green line denotes the energy error of SymUCCSD comparing to FCI energy vs. iteration numbers. The orange line denotes to energy error derived from CCSD vs. FCI and the green line indicates chemical accuracy with reference to FCI results(0.0016 Hartree).

Table II. The number of the excited configurations belongs to each irreps for C₂H₄.

| Irrep. | T_1 Num. | T_2 Num. |
|----------|------------|------------|
| A_g | 9 | 210 |
| B_{1g} | 8 | 176 |
| B_{2g} | 2 | 104 |
| B_{3g} | 5 | 110 |
| A_u | 2 | 104 |
| B_{1u} | 3 | 114 |
| B_{2u} | 11 | 182 |
| B_{3u} | 8 | 176 |
| Total | 48 | 1176 |

V. CONCLUSION

In this work, we have presented an algorithm to reduce the number of operators needed in UCCSD ansatz by employing the point group symmetry. The detailed derivation of this method is attached in Appendix VIB. After testing various molecules in different point groups using this method implemented in the MindQuantum simulator [42], we observed that molecules with higher symmetry such as D_{2h} could lead to

a larger reduction of the number of operators, meaning more compact quantum circuits. With the help of this scheme, we successfully simulated 28 qubits C_2H_4 molecule in reasonable computing resource, which is the largest molecule system simulated by VQE to date.

In principle, the point group symmetry is valid and non-exclusive for arbitrary molecular systems using UCC ansatz. It is naturally compatible with other methods based on excitation operators to compress further the quantum circuit depth, such as energy sorting scheme [21], (fermion or qubit) adapt VQE proposed by [16, 40, 41] or k-UpCCGSD [20]. Besides such algorithms inspired by the problems to reduce the quantum circuit depth, the quantum circuit compilation [48, 49] is also very important and inevitable to implement simulations of the molecule with chemical interests on real quantum hardware, such as superconducting or trapped ion systems.

To further enable even larger scale or more realistic chemistry simulation [50], one may treat the current method as a module and incorporate it into the deep VQE method [51, 52], the virtual quantum subspace expansion method [53], the quantum hybrid tensor network [54] and the quantum embedding methods such as density matrix embedding theory [55–57], and dynamical mean-field theory [58–60].

With the advancement of the aforementioned algorithms and the progress in quantum hardware, we anticipate a solid step towards the simulation of realistic molecular systems on the quantum computer soon.

ACKNOWLEDGEMENT

The authors gratefully thank Jinzhao Sun, Dr. Yifei Huang for helpful discussions.

-
- [1] R. P. Feynman, *Int. J. Theor. Phys.* **21**, 467 (1982).
- [2] A. Aspuru-Guzik, A. D. Dutoi, P. J. Love, and M. Head-Gordon, *Science* **309**, 1704 (2005).
- [3] I. Kassal, S. P. Jordan, P. J. Love, M. Mohseni, and A. Aspuru-Guzik, *PNAS* **105**, 18681 (2008).
- [4] J. Huh, G. G. Guerreschi, B. Peropadre, J. R. McClean, and A. Aspuru-Guzik, *Nat. Photonics* **9**, 615 (2015).
- [5] A. Peruzzo, J. McClean, P. Shadbolt, M.-H. Yung, X.-Q. Zhou, P. J. Love, A. Aspuru-Guzik, and J. L. O’Brien, *Nat. Commun.* **5**, 4213 (2014).
- [6] M.-H. Yung, J. Casanova, A. Mezzacapo, J. McClean, L. Lamata, A. Aspuru-Guzik, and E. Solano, *Sci. Rep.* **4**, 3589 (2014).
- [7] S. Endo, J. Sun, Y. Li, S. C. Benjamin, and X. Yuan, *Phys. Rev. Lett.* **125**, 010501 (2020).
- [8] P. J. J. O’Malley, R. Babbush, I. D. Kivlichan, J. Romero, J. R. McClean, R. Barends, J. Kelly, P. Roushan, A. Tranter, N. Ding, B. Campbell, Y. Chen, Z. Chen, B. Chiaro, A. Dunsworth, A. G. Fowler, E. Jeffrey, E. Lucero, A. Megrant, J. Y. Mutus, M. Neeley, C. Neill, C. Quintana, D. Sank, A. Vainsencher, J. Wenner, T. C. White, P. V. Coveney, P. J. Love, H. Neven, A. Aspuru-Guzik, and J. M. Martinis, *Phys. Rev. X* **6**, 031007 (2016).
- [9] A. Kandala, A. Mezzacapo, K. Temme, M. Takita, M. Brink, J. M. Chow, and J. M. Gambetta, *Nature* **549**, 242 (2017).
- [10] Y. Nam, J.-S. Chen, N. C. Pientis, K. Wright, C. Delaney, D. Maslov, K. R. Brown, S. Allen, J. M. Amini, J. Apisdorf, K. M. Beck, A. Blinov, V. Chaplin, M. Chmielewski, C. Collins, S. Debnath, K. M. Hudek, A. M. DuCore, M. Keesan, S. M. Kreikemeier, J. Mizrahi, P. Solomon, M. Williams, J. D. Wong-Campos, D. Moehring, C. Monroe, and J. Kim, *npj Quantum Information* **6**, 33 (2020).
- [11] G. A. Quantum, Collaborators, F. Arute, K. Arya, R. Babbush, D. Bacon, J. C. Bardin, R. Barends, S. Boixo, M. Broughton, B. B. Buckley, D. A. Buell, B. Burkett, N. Bushnell, Y. Chen, Z. Chen, B. Chiaro, R. Collins, W. Courtney, S. Demura, A. Dunsworth, E. Farhi, A. Fowler, B. Foxen, C. Gidney, M. Giustina, R. Graff, S. Habegger, M. P. Harrigan, A. Ho, S. Hong, T. Huang, W. J. Huggins, L. Ioffe, S. V. Isakov, E. Jeffrey, Z. Jiang, C. Jones, D. Kafri, K. Kechedzhi, J. Kelly, S. Kim, P. V. Klimov, A. Korotkov, F. Kostritsa, D. Landhuis, P. Laptev, M. Lindmark, E. Lucero, O. Martin, J. M. Martinis, J. R. McClean, M. McEwen, A. Megrant, X. Mi, M. Mohseni, W. Mruczkiewicz, J. Mutus, O. Naaman, M. Neeley, C. Neill, H. Neven, M. Y. Niu, T. E. O’Brien, E. Ostby, A. Petukhov, H. Putterman, C. Quintana, P. Roushan, N. C. Rubin, D. Sank, K. J. Satzinger, V. Smelyanskiy, D. Strain, K. J. Sung, M. Szalay, T. Y. Takeshita, A. Vainsencher, T. White, N. Wiebe, Z. J. Yao, P. Yeh, and A. Zalcman, *Science* **369**, 1084 (2020).
- [12] K. Yeter-Aydeniz, B. T. Gard, J. Jakowski, S. Majumder, G. S. Barron, G. Siopsis, T. S. Humble, and R. C. Pooser, *Adv. Quantum Technol.* **4**, 2100012 (2021).
- [13] P. Lolur, M. Rahm, M. Skogh, L. García-Álvarez, and G. Wendin, “Benchmarking the variational quantum eigensolver through simulation of the ground state energy of prebiotic molecules on high-performance computers,” (2020), [arXiv:2010.13578](https://arxiv.org/abs/2010.13578).
- [14] M. Kühn, S. Zanker, P. Deglmann, M. Marthaler, and H. Weiß, *J. Chem. Theory Comput.* **15**, 4764 (2019).
- [15] I. G. Ryabinkin, R. A. Lang, S. N. Genin, and A. F. Izmaylov, *J. Chem. Theory Comput.* **16**, 1055 (2020).
- [16] H. R. Grimsley, S. E. Economou, E. Barnes, and N. J. Mayhall, *Nat. Commun.* **10**, 3007 (2019).
- [17] P. L. Dallaire-Demers, J. Romero, L. Veis, S. Sim, and A. Aspuru-Guzik, *Quantum Sci. Technol.* **4**, 1 (2019), 1801.01053.
- [18] D. Wecker, M. B. Hastings, and M. Troyer, *Phys. Rev. A* **92**, 042303 (2015).
- [19] J. Romero, R. Babbush, J. R. McClean, C. Hempel, P. J. Love, and A. Aspuru-Guzik, *Quantum Sci. Technol.* **4**, 014008 (2018).
- [20] J. Lee, W. J. Huggins, M. Head-Gordon, and K. B. Whaley, *J. Chem. Theory Comput.* **15**, 311 (2019).
- [21] Y. Fan, C. Cao, X. Xu, Z. Li, D. Lv, and M.-H. Yung, “Circuit-depth reduction of unitary-coupled-cluster ansatz by energy sorting,” (2021), [arXiv:2106.15210](https://arxiv.org/abs/2106.15210).
- [22] S. Bravyi, J. M. Gambetta, A. Mezzacapo, and K. Temme, “Tapering off qubits to simulate fermionic hamiltonians,” (2017), [arXiv:1701.08213](https://arxiv.org/abs/1701.08213).
- [23] B. T. Gard, L. Zhu, G. S. Barron, N. J. Mayhall, S. E. Economou, and E. Barnes, *npj Quantum Inf.* **6**, 10 (2020), 1904.10910.

- [24] G. Greene-Diniz and D. Muñoz Ramo, *Int. J. Quantum Chem.* **121**, e26352 (2021).
- [25] P. Čárský, L. J. Schaad, B. A. Hess, M. Urban, and J. Noga, *J. Chem. Phys.* **87**, 411 (1987).
- [26] J. F. Stanton, J. Gauss, J. D. Watts, and R. J. Bartlett, *J. Chem. Phys.* **94**, 4334 (1991).
- [27] K. Setia, R. Chen, J. E. Rice, A. Mezzacapo, M. Pistoia, and J. D. Whitfield, *J. Chem. Theory Comput.* **16**, 6091 (2020).
- [28] K. Seki, T. Shirakawa, and S. Yunoki, *Phys. Rev. A* **101**, 052340 (2020).
- [29] T.-C. Yen, R. A. Lang, and A. F. Izmaylov, *J. Chem. Phys.* **151**, 164111 (2019).
- [30] F. Zhang, N. Gomes, N. F. Berthussen, P. P. Orth, C.-Z. Wang, K.-M. Ho, and Y.-X. Yao, *Phys. Rev. Research* **3**, 013039 (2021).
- [31] S. A. Fischer and D. Gunlycke, “Symmetry configuration mapping for representing quantum systems on quantum computers,” (2019), [arXiv:1907.01493](https://arxiv.org/abs/1907.01493).
- [32] S. McArdle, S. Endo, A. Aspuru-Guzik, S. C. Benjamin, and X. Yuan, *Rev. Mod. Phys.* **92**, 015003 (2020).
- [33] A. G. Taube and R. J. Bartlett, *Int. J. Quantum Chem.* **106**, 3393 (2006).
- [34] P. Jordan and E. P. Wigner, *The Collected Works of Eugene Paul Wigner*, 109 (1993).
- [35] M. Suzuki, *Commun. Math. Phys.* **51**, 183 (1976).
- [36] H.-Y. Huang, R. Kueng, and J. Preskill, (2021), [arXiv:2103.07510](https://arxiv.org/abs/2103.07510) [quant-ph].
- [37] T. Zhang, J. Sun, X.-X. Fang, X. Zhang, X. Yuan, and H. Lu, “Experimental quantum state measurement with classical shadows,” (2021), [arXiv:2106.10190](https://arxiv.org/abs/2106.10190) [quant-ph].
- [38] S. Hillmich, C. Hadfield, R. Raymond, A. Mezzacapo, and R. Wille, (2021), [arXiv:2105.06932](https://arxiv.org/abs/2105.06932) [quant-ph].
- [39] B. Wu, J. Sun, Q. Huang, and X. Yuan, (2021), [arXiv:2105.13091](https://arxiv.org/abs/2105.13091) [quant-ph].
- [40] H. L. Tang, V. Shkolnikov, G. S. Barron, H. R. Grimsley, N. J. Mayhall, E. Barnes, and S. E. Economou, *PRX Quantum* **2**, 020310 (2021).
- [41] Z.-J. Zhang, J. Sun, X. Yuan, and M.-H. Yung, (2020), [arXiv:2011.05283](https://arxiv.org/abs/2011.05283) [quant-ph].
- [42] Huawei, “Mindquantum,” Website (2021), <https://gitee.com/mindspore/mindquantum>.
- [43] N. Russell Johnson, in *The 4th Joint Meeting of the US Sections of the Combustion Institute* (2005).
- [44] Q. Sun, X. Zhang, S. Banerjee, P. Bao, M. Barbry, N. S. Blunt, N. A. Bogdanov, G. H. Booth, J. Chen, Z.-H. Cui, J. J. Eriksen, Y. Gao, S. Guo, J. Hermann, M. R. Hermes, K. Koh, P. Koval, S. Lehtola, Z. Li, J. Liu, N. Mardirossian, J. D. McClain, M. Motta, B. Mussard, H. Q. Pham, A. Pulkin, W. Purwanto, P. J. Robinson, E. Ronca, E. R. Sayfutyarova, M. Scheurer, H. F. Schurkus, J. E. T. Smith, C. Sun, S.-N. Sun, S. Upadhyay, L. K. Wagner, X. Wang, A. White, J. D. Whitfield, M. J. Williamson, S. Wouters, J. Yang, J. M. Yu, T. Zhu, T. C. Berkelbach, S. Sharma, A. Y. Sokolov, and G. K.-L. Chan, *J. Chem. Phys.* **153**, 024109 (2020).
- [45] Q. Sun, T. C. Berkelbach, N. S. Blunt, G. H. Booth, S. Guo, Z. Li, J. Liu, J. D. McClain, E. R. Sayfutyarova, S. Sharma, S. Wouters, and G. K.-L. Chan, *Wiley Interdiscip. Rev. Comput. Mol. Sci.* **8**, e1340 (2018).
- [46] J. P. Perdew, K. Burke, and M. Ernzerhof, *Phys. Rev. Lett.* **77**, 3865 (1996).
- [47] F. Weigend and R. Ahlrichs, *Phys. Chem. Chem. Phys.* **7**, 3297 (2005).
- [48] C. J. Trout and K. R. Brown, *Int. J. Quantum Chem.* **115**, 1296–1304 (2015).
- [49] T. Jones and S. C. Benjamin, “Quantum compilation and circuit optimisation via energy dissipation,” (2020), [arXiv:1811.03147](https://arxiv.org/abs/1811.03147) [quant-ph].
- [50] J. Sun, S. Endo, H. Lin, P. Hayden, V. Vedral, and X. Yuan, (2021), [arXiv:2106.05938](https://arxiv.org/abs/2106.05938) [quant-ph].
- [51] K. Fujii, K. Mitarai, W. Mizukami, and Y. O. Nakagawa, “Deep variational quantum eigensolver: a divide-and-conquer method for solving a larger problem with smaller size quantum computers,” (2020), [arXiv:2007.10917](https://arxiv.org/abs/2007.10917).
- [52] K. Mizuta, M. Fujii, S. Fujii, K. Ichikawa, Y. Imamura, Y. Okuno, and Y. O. Nakagawa, “Deep variational quantum eigensolver for excited states and its application to quantum chemistry calculation of periodic materials,” (2021), [arXiv:2104.00855](https://arxiv.org/abs/2104.00855).
- [53] T. Takeshita, N. C. Rubin, Z. Jiang, E. Lee, R. Babbush, and J. R. McClean, *Phys. Rev. X* **10**, 011004 (2020).
- [54] X. Yuan, J. Sun, J. Liu, Q. Zhao, and Y. Zhou, *Phys. Rev. Lett.* **127**, 040501 (2021).
- [55] G. Knizia and G. K.-L. Chan, *Phys. Rev. Lett.* **109**, 186404 (2012).
- [56] N. C. Rubin, “A hybrid classical/quantum approach for large-scale studies of quantum systems with density matrix embedding theory,” (2016), [arXiv:1610.06910](https://arxiv.org/abs/1610.06910).
- [57] Y. Kawashima, M. P. Coons, Y. Nam, E. Lloyd, S. Matsuura, A. J. Garza, S. Johri, L. Huntington, V. Senicourt, A. O. Maksymov, *et al.*, “Efficient and accurate electronic structure simulation demonstrated on a trapped-ion quantum computer,” (2021), [arXiv:2102.07045](https://arxiv.org/abs/2102.07045).
- [58] G. Kotliar, S. Y. Savrasov, K. Haule, V. S. Oudovenko, O. Parcollet, and C. A. Marianetti, *Rev. Mod. Phys.* **78**, 865 (2006).
- [59] B. Bauer, D. Wecker, A. J. Millis, M. B. Hastings, and M. Troyer, *Phys. Rev. X* **6**, 031045 (2016).
- [60] I. Rungger, N. Fitzpatrick, H. Chen, C. Alderete, H. Apel, A. Cowtan, A. Patterson, D. M. Ramo, Y. Zhu, N. H. Nguyen, *et al.*, “Dynamical mean field theory algorithm and experiment on quantum computers,” (2019), [arXiv:1910.04735](https://arxiv.org/abs/1910.04735).
- [61] F. A. Cotton, *Chemical applications of group theory* (John Wiley & Sons, 2003).
- [62] L. M. Falicov, *Am. J. Phys.* **35**, 782 (1967).

VI. APPENDIX

A. Point group

The point group is a set of symmetry operations under which the object is indistinguishable from the original geometry. In this paper, we mainly refer the object as a molecule. The so-called point group comes from the origin point being unchanged with arbitrary symmetry operation since all the symmetry elements intersect at it [61, 62].

The symmetry operations include reflection, inversion, rotation and identity operation, which correspond to symmetry elements of mirror planes σ , inversion center i , rotation axes C_n and identities E , respectively. Molecules belong to a symmetry point group if it is unchanged under all the symmetry operations of this group.

In application, the character table and the product table are the essential and frequently used devices for the point group. Table. 6 is a typical character table of D_{2h} group, in which the rows are the irreducible group representations and the

columns are the conjugacy class of the symmetric operations. The table entries are the characters (trace of the matrix) of the symmetric operations under the different irreducible representations. Fig. 1a is the product table of D_{2h} group, which exhibits how the character changes under the direct product of the representations. Since the characters of the representation of a direct product are equal to the products of the characters of the representations based on the individual sets of functions, the product table of the point group can be generated by the products of the characters.

Taking the direct product of B_{1g} and B_{2g} as an example, the characters of B_{1g} are 1, -1, -1, 1, 1, 1, -1, -1 and B_{2g} are 1, -1, 1, -1, 1, -1, 1, -1. The products of the characters under each conjugacy class of the group element are 1, 1, -1, -1, 1, -1, -1, 1, respectively, which correspond to the characters of B_{3g} irreducible representation. So the direct product of B_{1g} and B_{2g} leads to B_{3g} . Similarly, a product table of D_{2h} group is constructed according to the result of the direct product between two arbitrary irreps. Here we take BeH_2 as an example to illustrate detailed steps for our algorithm.

BeH_2 structure belongs to the $D_{\infty h}$ group, which is non-abelian. In this paper, we only discuss the abelian situation which is easy to handle. Here, we take the D_{2h} , an Abelian subgroup of $D_{\infty h}$ with the highest rank, to reduce the parameters of BeH_2 . The Cartesian coordinate system is set up with the origin at Be atom and the z-axis along Be-H as shown in Fig. 7.

There are eight symmetry operations corresponding to the same number of symmetry elements for BeH_2 under D_{2h} group. Three C_2 rotation axes are along the x-, y-, z-axis, and three mirrors are in the xy-, yz-, zx- planes which are perpendicular with each other and intersect in a C_2 rotation axis. The rest of the symmetry elements are the inversion center at the place of Be atom and the identity. We take the molecular orbital of BeH_2 as the example to demonstrate how to understand the spatial symmetry in it combining with the character table.

The isosurface of the wavefunction of molecular orbital are given in Fig. 8, in which the blue surface represents the positive value, and the red surface represents the negative one. The character in character Table. 6 indicates how the sign of the certain irreducible representation changes under the par-

| D_{2h} | E | $C_2(x)$ | $C_2(y)$ | $C_2(z)$ | i | $\sigma(xy)$ | $\sigma(xz)$ | $\sigma(yz)$ |
|----------|---|----------|----------|----------|---|--------------|--------------|--------------|
| A_g | 1 | 1 | 1 | 1 | 1 | 1 | 1 | 1 |
| B_{1g} | 1 | -1 | -1 | 1 | 1 | 1 | -1 | -1 |
| B_{2g} | 1 | -1 | 1 | -1 | 1 | -1 | 1 | -1 |
| B_{3g} | 1 | 1 | -1 | -1 | 1 | -1 | -1 | 1 |
| A_u | 1 | 1 | 1 | 1 | 1 | -1 | -1 | -1 |
| B_{1u} | 1 | -1 | -1 | 1 | 1 | -1 | 1 | 1 |
| B_{2u} | 1 | -1 | 1 | -1 | 1 | 1 | -1 | 1 |
| B_{3u} | 1 | 1 | -1 | -1 | 1 | 1 | 1 | -1 |

Fig. 6. The character table of D_{2h} group for BeH_2 .

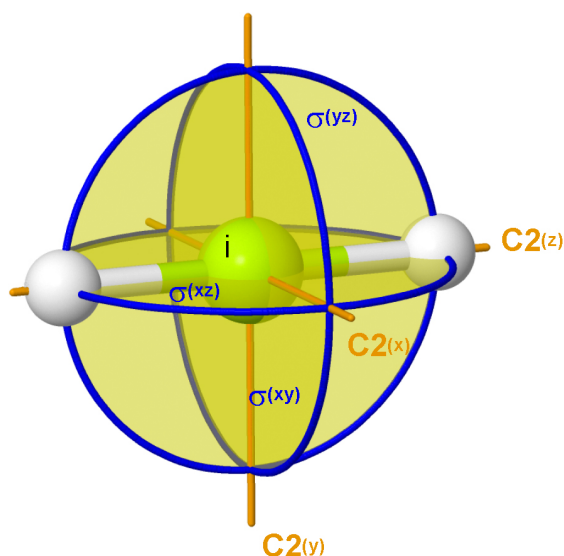


Fig. 7. The symmetry elements of BeH_2 in D_{2h} point group.

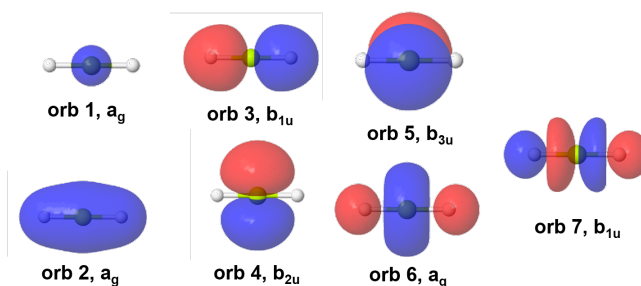


Fig. 8. The isosurface of the wavefunction of molecular orbital (isovalue is 0.03 a.u.).

ticular symmetry operation. For the A_g orbitals, the sign of the wavefunction maintains under arbitrary symmetry operation. Thus, all the characters are 1. For the B_{1u} orbitals like orb 3 and orb 7, the sign of the wavefunction is kept after rotated along z-axis or reflected by xz-plane and yz-plane. But the sign exchanges after rotated by x-axis and y-axis or reflected by xy-plane. Thus, the characters are -1 for i, $C_2(x)$, $C_2(y)$ and $\sigma(xy)$ while +1 for the other operations. The product table is then generated according to the character table as shown in Fig. 1a. Then it is possible to get the irrep of the excited states.

In total, there are 12 single excited states and 78 double excited states for BeH_2 . Only 23 excitations shared the same irreducible representation A_g as the reference state. Thus, the amplitudes of the certain 23 excited states are considered to construct the ansatz and optimized in the following VQE steps.

B. Validation of the Point Group Symmetry Reduction in UCC

Here we give a short proof to valid the algorithm. In the UCC theory, the wavefunction of a chemical system $|\Psi\rangle$ is constructed from the reference wavefunction $|\Psi_0\rangle$, which is usually a Hartree-Fock Slater determinant, by applying $e^{\hat{T}-\hat{T}^\dagger}$ as

$$|\Psi\rangle = e^{\hat{T}-\hat{T}^\dagger} |\Psi_0\rangle, \quad (11)$$

and the Schrödinger equation can be written as

$$\hat{H}|\Psi\rangle = E_{ucc}|\Psi\rangle. \quad (12)$$

For ensuring $|\Psi\rangle$ to be a solution of the Schrödinger equation, the cluster operator $e^{\hat{T}-\hat{T}^\dagger}$ here is not arbitrary but has to satisfy some conditions. In the following we will present how to reduce the number of operators and terms in the unitary coupled cluster wavefunction $|\Psi\rangle$. Note that the wavefunction here refers to a solution of the Schrödinger equation instead of a quantum state prepared on a quantum computer.

Here we have assumed that both $|\Psi_0\rangle$ and $|\Psi\rangle$ are non-degenerated states. For a symmetry operation \hat{R}_i belongs to an Abelian point group G , the Hamiltonian is commute with it, $\hat{H}\hat{R}_i = \hat{R}_i\hat{H}$. Thus we have

$$\hat{H}\hat{R}_i|\Psi\rangle = \hat{R}_i\hat{H}|\Psi\rangle = E_{ucc}\hat{R}_i|\Psi\rangle = E_{ucc}(\hat{R}_i|\Psi\rangle) \quad (13)$$

It indicates that $\hat{R}_i|\Psi\rangle$ is also the eigenstate of the Hamiltonian. So we come to

$$\exists \gamma : \hat{R}_i|\Psi\rangle = \gamma|\Psi\rangle \quad (14)$$

where the value of γ is the irreducible character that can be looked up from the character table of the corresponding point group. The irreducible characters in the Abelian point group are always 1 or -1.

Next, we use indirect proof to show that $|\Psi_0\rangle$ and $|\Psi\rangle$ belong to the same irrep:

$$D(|\Psi_0\rangle) = D(|\Psi\rangle) \quad (15)$$

where D is the irrep of the corresponding wavefunction.

If we assume that

$$\exists \hat{R}_i \in G : \hat{R}_i|\Psi_0\rangle = c_0|\Psi_0\rangle, \hat{R}_i|\Psi\rangle = c|\Psi\rangle, c_0 \neq c \quad (16)$$

On the other side, by applying the symmetry operator to $|\Psi_0\rangle$ and $|\Psi\rangle$ respectively, we have

$$\langle \Psi_0 | \Psi \rangle = \langle \Psi_0 | \hat{R}^\dagger \hat{R} | \Psi \rangle = c_0 c_1 \langle \Psi_0 | \Psi \rangle \quad (17)$$

We note that a reasonable solution $|\Psi\rangle$ perturbed from $|\Psi_0\rangle$ should be overlapping with the Hartree-Fock determinant $|\Psi_0\rangle$ [33]

$$\langle \Psi_0 | \Psi \rangle \neq 0 \quad (18)$$

It indicates that

$$c_0 c = 1 \quad (19)$$

In an Abelian point group, the characters are either 1 or -1. So we know

$$c_0 = c, \quad (20)$$

which is contradictory to the assumption, and it means that

$$\forall \hat{R}_i \in G : \hat{R}_i|\Psi_0\rangle = c_i|\Psi_0\rangle, \hat{R}_i|\Psi\rangle = c_i|\Psi\rangle. \quad (21)$$

This concludes that each symmetry operation $\hat{R}_i \in G$ acting on $|\Psi\rangle$ and $|\Psi_0\rangle$ will lead to the same character, and thus they belong to the same *irrep*.

$$D(|\Psi_0\rangle) = D(|\Psi\rangle) \quad (22)$$

By using Taylor expansion to the cluster operator $e^{\hat{T}-\hat{T}^\dagger}$, $|\Psi\rangle$ can be written as the linear combination of Slater determinants:

$$|\Psi\rangle = k(|\Psi_0\rangle) + \sum_{i,a} t_i^a |\Psi_i^a\rangle + \sum_{i,j,a,b} t_{ij}^{ab} |\Psi_{ij}^{ab}\rangle + \dots, \quad (23)$$

where k is the normalized coefficient. As we have presented that the $|\Psi\rangle$ and $|\Psi_0\rangle$ are of the same irrep, so all the terms in the expansion are required to have the same irrep as the reference wavefunction. If $D(t_i^a |\Psi_i^a\rangle) \neq D(|\Psi_0\rangle)$, $t_i^a |\Psi_i^a\rangle$ must be ZERO. So are the double and higher excited terms.